The Journal of Physical Chemistry

 VOLUME 97, NUMBER 25, JUNE 24, 1993

LETTERS

Effects of Chemically-Bound, Flexible Hydrocarbon Species on the Frictional Properties of Diamond Surfaces

J. A. Harrison,* C. T. White, R. J. Colton, and D. W. Brenner

Chemistry Division, Code 6179, Naval Research Laboratory, Washington, D.C. 20375-5342

Received: February 10, 1993; In Final Form: April 23, 1993

We have used molecular dynamics simulations to examine friction when two diamond (111) surfaces are placed in sliding contact. We find that flexible hydrocarbon species, chemically bound to the diamond surface, can lead to a significant reduction of the calculated friction at high loads. In addition to clarifying the effects of such species on atomic-scale friction at diamond interfaces, these simulations might also yield insight into more complicated systems, e.g., Langmuir–Blodgett films, and aid in the design of low-friction coatings.

The friction and wear of surfaces are two of the more costly problems facing industry today. Liquid lubricants and boundary layer additives are widely used to reduce wear and increase equipment lifetime. There are, however, many applications, such as those dealing with the vacuum of outer space and those at high or low temperatures, where liquid lubricants cannot be used. As a result, some solid-state materials, such as molybdenum disulfide and diamond, that can be deposited as thin films have become important tribological materials.

Diamond and diamond films deposited by chemical vapor deposition (CVD) show relatively low friction and wear.[1-6] While inroads have been made into the qualitative understanding of friction and wear on the macroscopic scale,[4-6] little is known about them on the atomic scale. Recent advances in scientific instrumentation have allowed, for the first time, the study of atomic-scale friction and wear leading to the emergence of a new field called nanotribology.[7] For example, the surface force apparatus has been used to study the rheology of molecularly thin liquid layers,[8-11] a quartz crystal microbalance has been used to measure the sliding friction of molecularly thin adsorbed films,[12,13] and the atomic force microscope (AFM) has been used to measure the frictional force between a sharp tip (possibly a single asperity) and a flat surface during sliding.[14-19] These innovative experiments have also stimulated theoretical work. For instance, atomic-scale friction has been investigated computationally using analytical models,[20-23] first principles calculations,[24-26] and molecular dynamics.[27-32]

In this letter, we use molecular dynamics simulations to investigate the atomic-scale friction between two diamond (111) surfaces in sliding contact. Our previous work focused on the behavior of the friction coefficient, μ, as a function of normal load, temperature, crystallographic sliding direction, and sliding speed for two atomically-flat, hydrogen-terminated diamond (111) surfaces.[31] This new work examines effects on atomic-scale friction caused by replacing $^1/_8$ of the hydrogen atoms on one diamond surface with either methyl, ethyl, or *n*-propyl groups. The larger, more flexible hydrocarbon groups are found to act as a physical and, perhaps, chemical barrier between the sliding surfaces reducing μ at higher loads by a factor of 1.5–2 compared to the completely hydrogen-terminated system.

The molecular dynamics sliding experiment is briefly described below; the details have been given elsewhere.[31,32] A typical starting configuration is shown in Figure 1. In this case, two hydrogen atoms of the upper surface have been replaced by ethyl groups. (In this work, the effect of chemically-bound, flexible groups was examined by replacing two hydrogen atoms with methyl, ethyl, or *n*-propyl groups in these same two locations.) The two outermost layers of the top and bottom lattices (Figure 1a) are held rigid, and their relative position is used to define the distance between the two inner surfaces. Experimentally, normal load, rather than distance, is held constant to maintain a constant

* To whom correspondence should be addressed.

0022-3654/93/2097-6573$04.00/0

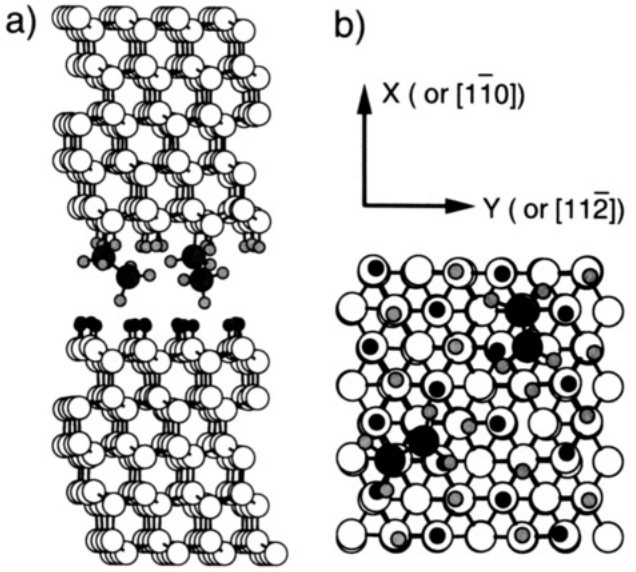

Figure 1. Typical starting configuration for one of the ethyl-terminated diamond (111) surfaces examined here. The large open circles represent carbon atoms, the large gray balls represent carbon atoms of the chemically-bound ethyl groups, the small light-gray balls represent hydrogen atoms, and the small dark-gray balls represent lower-surface hydrogen atoms. The system is viewed along the [$\bar{1}$10] direction and the [111] direction in (a) and (b), respectively. In (b) the carbon atoms of the upper lattice are not shown.

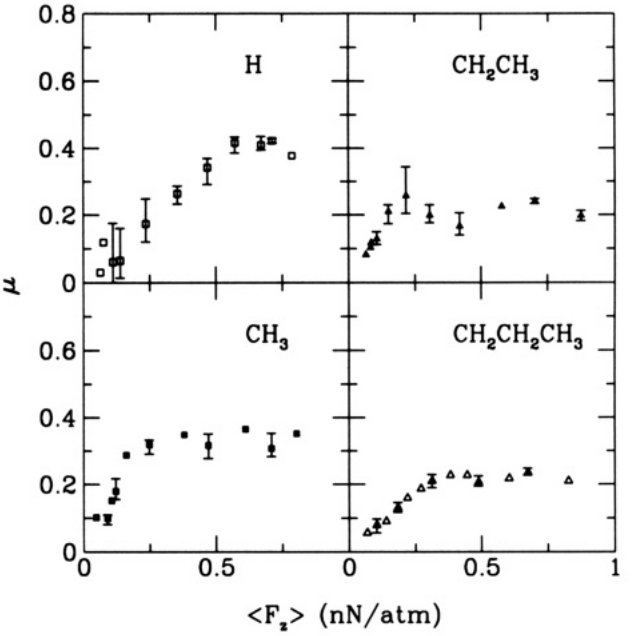

Figure 2. Average friction coefficient as a function of average normal load, $\langle F_z \rangle$, per atom for sliding in the [11$\bar{2}$] crystallographic direction at 1.0 Å/ps and 300 K. Open squares, filled squares, filled triangles, and open triangles represent the hydrogen-, methyl-, ethyl-, and *n*-propyl-terminated systems, respectively.

contact area. In these simulations, the contact area does not vary appreciably with the addition of the hydrocarbon groups. The sliding is simulated by moving the rigid layers of the upper surface at a constant velocity (1.0 Å/ps) in the chosen sliding direction. The remaining atoms are allowed to dynamically evolve in time according to Newton's equations of motion. The forces governing their motion are derived from an empirical hydrocarbon potential.[33-35] The temperature of the system is maintained at 300 K by applying a thermostat to the middle five layers of each lattice.[36] Periodic boundary conditions are applied in the plane of the surfaces, simulating an infinite interface.

In this letter, we report average friction coefficients as a function of average normal load at 300 K for sliding the upper surface in the [11$\bar{2}$] crystallographic direction. The normal load is increased by decreasing the separation between the rigid layers. The friction coefficient, for an individual sliding run, is taken to be the average frictional force (average force in the direction of sliding) on the rigid layers of the upper lattice divided by the average normal force on those same rigid layers.[31,32] The average friction coefficients are obtained by averaging over sliding simulations whose starting configurations differ in horizontal position of the upper surface.

The friction coefficients for each system are plotted in Figure 2 as a function of average normal load per atom. Those data points that have lines extending above and below them represent friction coefficients which are the average of three independent starting configurations that differ by the horizontal position of the upper surface. In addition to the original horizontal position of the upper surface (Figure 1b), the two other starting configurations are obtained by two successive translations of the upper surface from its original horizontal position by 0.5 Å in the [1$\bar{1}$0] crystallographic direction (the direction perpendicular to the sliding direction) between sliding runs. Because the repeat distance in the [1$\bar{1}$0] direction is approximately 2.5 Å and it is bisected by a mirror plane, these three starting configurations span the repeat distance in the [1$\bar{1}$0] crystallographic direction. To obtain better statistics, the two starting configurtions which are 0.25 and 0.75 Å from the mirror plane (the mirror plane is 1.25 Å from the original starting configuration) were averaged with sliding runs which are equidistant from, and on the other side of, the mirror plane. For example, the data from the starting configuration which is 0.25 Å from the mirror plane was averaged with data from a run whose starting configuration was –0.25 Å from the mirror plane. These two averaged data points were then averaged with the data from the sliding run where the upper surface was in its original horizontal position. The upper and lower lines drawn from these points extend to the maximum and minimum friction coefficients obtained from these three independent data points, respectively. Thus, the lines represent the range of friction coefficients obtained at a given load. Data points which do not have lines extending from them are the friction coefficients calculated from one sliding run, where the upper surface is in the horizontal position relative to the lower surface shown in Figure 1a.

For the completely hydrogen-terminated system, μ increases with increasing load with the range of μ values being larger at lower loads than at higher loads. Both of these observations are governed by the atomic-scale sliding mechanisms, which are apparent from animated sequences of these simulations. The way in which the atomic-scale sliding mechanisms govern the behavior of μ with load has been described elsewhere.[31] Briefly, as the upper surface slides in the [11$\bar{2}$] crystallographic direction, the hydrogen atoms on the upper and lower surfaces encounter each other. Animated sequences confirm that these encounters give rise to vibrational excitation of the hydrogen atoms. The hydrogen atoms subsequently impart this energy to the rest of the lattice. This dissipation of energy is the essence of the atomic-scale friction process. As the load increases, so does the vibrational excitation of the hydrogen atoms; thus, friction increases.

The varying size of the range of calculated μ values is related to the atomic-scale sliding mechanisms in the following way. There are approximately two types of horizontal starting configurations, those for which the hydrogen atoms of both the upper and the lower surfaces lie along the same line in the [11$\bar{2}$] crystallographic direction and those where they do not. For those configurations where the hydrogen atoms lie along the same line, if the upper surface were held rigid as it slides, the hydrogen atoms of the upper surface would pass directly over the top of the lower surface hydrogen atoms. Because the upper surface atoms are allowed to dynamically evolve in time, the hydrogen atoms are able to move to reduce the strength of this interaction. Animated sequences show that the hydrogen atoms of the upper

surface revolve around the lower surface hydrogen atoms as the surface slides.[31]

For those configurations where the hydrogen atoms of both surfaces do not lie along a line in the [11$\bar{2}$] crystallographic direction, the hydrogen atoms of the upper surface travel in the space between adjacent hydrogen atom rows on the lower surface: thus, avoiding the situation where they would have to pass directly over the lower surface hydrogen atoms. This type of starting configuration almost always results in lower friction coefficients than the configuration where the hydrogen atoms lie in a line. For the smallest loads examined, this starting configuration yielded values of μ which were approximately zero, while the other starting configuration yielded nonzero values of μ. Therefore, for very low loads, the range of μ values is fairly large. As the load is increased, the surfaces are closer together and the interaction between hydrogen atoms increases regardless of starting configuration; thus, the range of μ values obtained decreases.

When methyl groups are substituted for two hydrogen atoms on the upper surface the behavior of μ with load is similar to that observed for the completely hydrogen-terminated case. At low loads, the average value of μ is slightly larger and the range of μ values is slightly smaller, compared to the completely hydrogen-terminated case. The range of μ values is smaller in this case because of the size of the methyl groups compared to the size of the hydrogen atoms. Even when the upper surface is in the configuration where the hydrogen atoms of the upper and lower surfaces do not lie in a line along the [11$\bar{2}$] crystallographic direction, the size of the methyl groups prevents them from traveling between adjacent hydrogen atom rows with a negligible interaction. Also, for both types of horizontal starting configurations, in addition to the interaction with lower surface hydrogen atoms the methyl groups interact with the second layer carbon atoms.[32] It is these additional interactions of the methyl groups that are responsible for the increased average value of μ and the decreased range of μ values obtained at low loads. For loads up to 0.25 nN/atom, μ increases with load. For loads between 0.25 and 0.8 nN/atom, μ remains nearly constant as the load is increased. At loads greater than 0.4 nN/atom, the friction coefficients are slightly less than those for the completely hydrogen-terminated system. However, adding a larger, more flexible group such as ethyl to the upper surface causes a markedly different effect at high loads. For loads up to 0.4 nN/atom, the friction coefficients are comparable to the completely hydrogen-terminated system. In contrast, for loads larger than approximately 0.4 nN/atom, μ is much lower than for the completely hydrogen-terminated system and becomes nearly constant.

Visualizing the molecular dynamics simulation gives some insight into how the motion of the ethyl groups affects μ. Because the ethyl group is larger and more flexible than a hydrogen atom, it can bend and move. For example, loading the surface causes the ethyl group to bend over and lie down on the surface between the lower-surface hydrogen atoms. At low loads, sliding the surfaces causes the ethyl grops to move into positions analogous to dragging a short chain, i.e., the tail follows the tethered point. For the type of horizontal starting configuration where the upper surface and the lower surface interface atoms lie along a line in the [11$\bar{2}$] crystallographic direction, this motion is illustrated in Figure 3 by plotting the position of the terminal part of the ethyl group (dark line) on a potential energy contour plot of the hydrogen-terminated diamond (111) lower surface. The dashed lines represent the attachment points of the ethyl groups on the upper surface. The terminal group moves from its initial position (indicated by the dark triangle) to fall in behind the bonded end of the molecule (closer to the attachment point). The sliding causes the tethered group to pass directly over the hydrogen atoms on the lower surface that are in the sliding path, essentially the same path taken by the completely hydrogen-terminated surface. Thus, at these loads, the interaction between the surfaces is

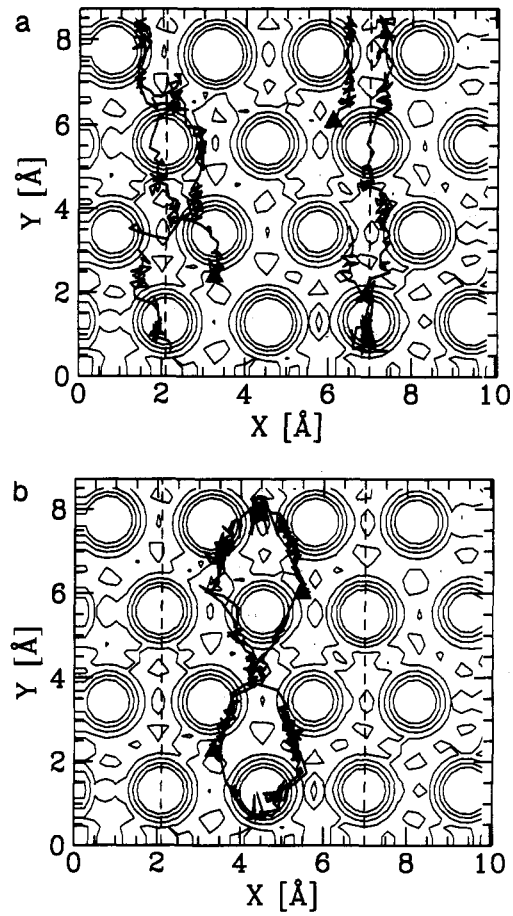

Figure 3. Center of mass trajectories of the CH_3 portion of the ethyl groups (solid line) plotted on a potential energy contour map of a hydrogen-terminated diamond (111) surface. The sliding direction is from the bottom of the figure to the top of the figure. Due to the periodic boundary conditions, trajectories which disappear off the plot at large Y reappear at the bottom of the figure (near Y=0). This contour map was generated by rastering a hydrogen atom, which is approximately 0.6 Å above the diamond surface, across the surface in X and Y. The filled triangles represent the starting points of the individual CH_3 entities. The dashed line represents the attachment point of the ethyl group on the upper surface. The average normal force per atom on the rigid layer atoms of the upper surface is 0.065 nN in (a) and 0.42 nN in (b). The contour values are 0.271, 0.771, 1.271, 1.771, and 2.271 eV.

approximately the same as that in the completely hydrogen-terminated system; hence, μ is approximately the same. For this same type of horizontal starting configuration at loads greater than 0.4 nN/atom, the tail of the ethyl group does not usually follow the tethered point but rather uses its flexibility to detour around the high potential energy barriers (Figure 3b)—in effect smoothing the surface and hence reducing the observed μ. The flexibility of the ethyl groups also allows the free end of the tethered group to travel in potential energy valleys when the interface atoms do not lie initially along a line in the [11$\bar{2}$] crystallographic direction.

Similarly, the friction coefficient found for the *n*-propyl system depends on the conformation of the *n*-propyl group and the path it takes during sliding. Due to its larger size, its flexibility, and the spacing between the lower-surface hydrogen atoms (in the [11$\bar{2}$] crystallographic direction), under load, it adopts a bent conformation when sliding that minimizes repulsive interactions. This conformation is relatively stable and does not change unless higher loads are applied. By this point, μ has become independent of load and has reached a value comparable to that obtained in the ethyl-terminated system.

In summary, over the entire load range examined, μ increases with load for the hydrogen-terminated system. The methyl-terminated system behaves much the same way except at larger

loads where μ remains relatively constant. For the ethyl and *n*-propyl-terminated systems, μ increases with load for small loads; but, at higher loads, μ for these more flexible species becomes independent of load and is significantly reduced from what it was for the completely hydrogen-terminated system.

Due to experimental scale lengths, poorly characterized interaction geometries, and sampe cleanliness, it is difficult to compare these data directly with current experimental results. For example, for the hydrogen-terminated system the trend of increasing μ with increasing load agrees with the recent AFM experiments of Mate,[17] where a tungsten tip was slid over a hydrogen-terminated diamond (111) surface. However, comparison of these experiments to our simulations is difficult since these experiments were carried out in air where surface contamination is present. To date, the experiment which most closely resembles the simulation conditions is the ultrahigh vacuum AFM data of German et al.[16] In that work, they measured a frictional force for a CVD diamond tip sliding on a hydrogen-terminated diamond (111) surface which was independent of load. These data apparently contradict our results for the hydrogen-terminated system; however, by comparing the shape and magnitude of the attractive force upon tip–sample retraction and approach, German et al. concluded that the sample or tip may be covered by some physisorbed or chemisorbed species. Our simulations show that adsorbed species can have profound effects on the dependence of the friction coefficient with load.

If we consider the hydrocarbon systems studied here as precursors to a full Langmuir–Blodgett (LB) film, the simulations predict a reduction in friction in the presence of flexible species chemically-bound to the diamond surface. This is consistent with the reduction of friction with the addition of LB films[18,19] observed in recent AFM experiments. Thus, these and future simulations might provide some insight into the frictional behavior of boundary layer films and, perhaps, ultimately aid in the design of low-friction coatings.

Acknowledgment. This work was partially supported by the Office of Naval Research under Contract N00014-92-WX-24183. J.A.H. would like to thank D. H. Robertson for his help with the preparation of Figure 1, C. M. Mate for helpful discussions and prepublication access to his data, and the ASEE and the Office of Naval Research for support.

References and Notes

(1) Hayward, I. P.; Singer, I. L.; Seitzman, L. E. *Wear* **1992**, *157*, 215.
(2) Miyoshi, K.; Wu, R. L. C.; Garscadden, A. *Surf. Coat. Tech.* **1992**, *54/55*, 428.
(3) Kohzaki, M.; Higuchi, K.; Noda, S.; Uchida, K. *J. Mater. Res.* **1992**, *7*, 1769.
(4) Tabor, D. In *Properties of Diamond*; Field, J. E., Ed.; Academic Press: London, 1979; pp 325–350.
(5) Enomoto, Y.; Tabor, D. *Proc. R. Soc. London A* **1981**, *373*, 405.
(6) Samuels, B.; Wilks, J. *J. Mater. Sci.* **1988**, *23*, 2846.
(7) Granick, S. *Mater. Res. Bull.* **1991**, *16*, 33.
(8) Chen, Y.-L.; Israelachvilli, J. N. *J. Phys. Chem.* **1992**, *96*, 7752. Yoshizawa, H.; Chen, Y.-L.; Israelachvilli, J. N. *Wear*, in press.
(9) Israelachvilli, J. N.; McGuiggan, P. M.; Homola, A. M. *Science* **1988**, *240*, 189.
(10) Van Alsten, J.; Granick, S. *Phys. Rev. Lett.* **1991**, *16*, 33.
(11) Granick, S. *Science* **1991**, *283*, 1374.
(12) Krim, J.; Solina, D. H.; Chiarello, R. *Phys. Rev. Lett.* **1991**, *66*, 181.
(13) Watts, E. T.; Krim, J.; Windom, A. *Phys. Rev. B* **1990**, *41*, 3466.
(14) Mate, C. M.; McClelland, G. M.; Erlandsson, R.; Chiang, S. *Phys. Rev. Lett.* **1987**, *59*, 1942.
(15) Erlandsson, R.; Hadziloannou, G.; Mate, C. M.; McClelland, G. M.; Chiang, S. *J. Chem. Phys.* **1988**, *89*, 5190.
(16) German, G. J.; Cohen, S. R.; Neubauer, G.; McClelland, G. M.; Seki, H. *J. Appl. Phys.* **1993**, *73*, 163.
(17) Mate, C. M. *Wear*, in press.
(18) Meyer, E.; Overney, R.; Brodbeck, D.; Howald, L.; Luthi, R.; Frommer, J.; Guntherodt, H.-J. *Phys. Rev. Lett.* **1992**, *69*, 1777.
(19) Meyer, E.; Overney, R.; Luthi, R.; Brodbeck, D.; Howald, L.; Frommer, J.; Guntherodt, H.-J.; Wolter, O.; Fujihira, M.; Takano, H.; Gotoh, Y. *Thin Solid Films* **1992**, *220*, 132.
(20) Tomlinson, G. A. *Philos. Mag. Ser.* **1929**, *7*, 905.
(21) Frenkel, F. C.; Kontorova, T. *Zh. Eksp. Teor. Fiz.* **1938**, *8*, 1340.
(22) Hirano, M.; Shinjo, K. *Phys. Rev. B* **1984**, *41*, 11837.
(23) Hirano, M.; Shinjo, K.; Kaneko, R.; Murata, R. *Phys. Rev. Lett.* **1991**, *67*, 2642.
(24) Sokoloff, J. B. *Surf. Sci.* **1984**, *144*, 267.
(25) Sokoloff, J. B. *Phys. Rev. B* **1990**, *42*, 760.
(26) Zhong, W.; Tomanek, D. *Phys. Rev. Lett.* **1990**, *64*, 3054.
(27) McClelland, G. M.; Glosli, J. N. NATO ASI Proceedings on *Fundamentals of Friction: Macroscopic and Microscopic Processes*; Singer, I. L., Pollock, H. M., Eds.; Kluwer Academic Publishers: Dordrect, 1992; pp 405–426.
(28) Landman, U.; Luedtke, W. D. *J. Vac. Sci. Technol. B* **1991**, *9*, 414.
(29) Thompson, P. A.; Robbins, M. O. *Phys. Rev. Lett.* **1989**, *63*, 766.
(30) Thompson, P. A.; Robbins, M. O. *Science* **1990**, *250*, 792.
(31) Harrison, J. A.; White, C. T.; Colton, R. J.; Brenner, D. W. *Phys. Rev. B* **1992**, *46*, 9700.
(32) Harrison, J. A.; White, C. T.; Colton, R. J.; Brenner, D. W. *Wear*, in press.
(33) Brenner, D. W. *Phys. Rev. B* **1990**, *42*, 9458.
(34) Brenner, D. W.; Harrison, J. A.; White, C. T.; Colton, R. J. *Thin Solid Films* **1991**, *206*, 220.
(35) Harrison, J. A.; White, C. T.; Colton, R. J.; Brenner, D. W. *Thin Solid Films* **1991**, *206*, 213.
(36) Berendsen, H. J. C.; Postma, J. P. M.; van Gunsteren, W. F.; DiNola, A.; Haak, J. R. *J. Chem. Phys.* **1984**, *81*, 3684.